JOURNAL PRE-PROOF

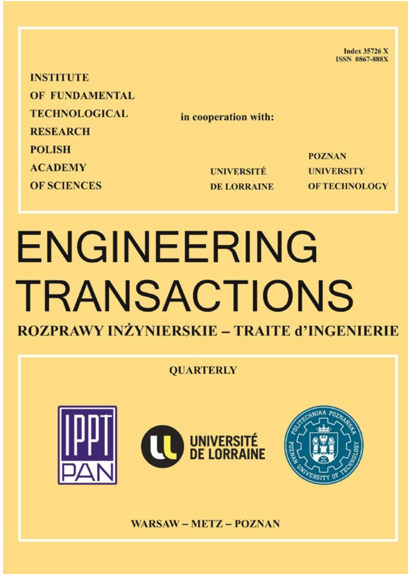

This is an early version of the article, published prior to copyediting, typesetting, and editorial correction. The manuscript has been accepted for publication and is now available online to ensure early dissemination, author visibility, and citation tracking prior to the formal issue publication.

It has not undergone final language verification, formatting, or technical editing by the journal's editorial team. Content is subject to change in the final Version of Record.

To differentiate this version, it is marked as "PRE-PROOF PUBLICATION" and should be cited with the provided DOI. A visible watermark on each page indicates its preliminary status.

The final version will appear in a regular issue of *Engineering Transactions*, with final metadata, layout, and pagination.

Title: Simulation of Vibro-Isolation Performance For Sensitive Cargo Transportation on Planforms with Quasi-Zero Stiffness Suspension Under Impact Perturbations

Author(s): Oleksiy LARIN, Ksenia POTOPALSKA, Galina TIMCHENKO, Nikita VASYLCHENKO

DOI: https://doi.org/10.24423/engtrans.2025.3484

Journal: *Engineering Transactions*

ISSN: 0867-888X, e-ISSN: 2450-8071

Publication status: In press

Received: 2024-12-13

Revised: 2025-06-01

Accepted: 2025-07-14

Published pre-proof: 2025-12-16

Please cite this article as:

Larin O., Potopalska K., Timchenko G., Vasylchenko N., Simulation of Vibro-Isolation Performance For Sensitive Cargo Transportation on Planforms with Quasi-Zero Stiffness Suspension Under Impact Perturbations, *Engineering Transactions*, 2025, https://doi.org/10.24423/engtrans.2025.3484

Simulation of Vibro-Isolation Performance For Sensitive Cargo Transportation on Planforms with Quasi-Zero Stiffness Suspension Under Impact Perturbations

Oleksiy LARIN(1)* 0000-0002-5721-4400, Ksenia POTOPALSKA(1) 0000-0001-8184-4229, Galina TIMCHENKO(2) 0000-0002-7279-7173, Nikita VASYLCHENKO(1)

(1) Department of Mathematical Modeling and Intelligent Computing in Engineering
(2) Department of Applied Mathematics

National Technical University "Kharkiv Polytechnic Institute", Kharkiv, Ukraine

*Corresponding Author e-mail: oleksiy.larin@khpi.edu.ua

This work deals with the theoretical modeling of the vertical dynamics of a specialized vehicle featuring a dual suspension system. Vehicle ride quality is essential for ensuring the safety and comfort of passengers and the protection of sensitive or hazardous cargo. The study focuses on a two-axle vehicle model with a dual suspension system. The first level comprises a traditional suspension with linear stiffness, while the second level features nonlinear quasi-zero stiffness (QZS) characteristics. The research employs a discrete nonlinear dynamic model considers the vertical displacements and angular rotations of the vehicle's masses. The nonlinear QZS response is modeled to optimize vibration isolation performance under varying load conditions, while damping effects are included via a Rayleigh dissipation function. The integral characteristics of the QZS element are also studied in detail using finite element (FE) computer simulations in a 3D statement. These simulations provide a comprehensive understanding of the mechanical response and stress-strain distribution within the QZS element, validating its performance under real-world conditions. The results demonstrate the influence of the nonlinear suspension characteristics on the vibration isolation performance and load stability. The QZS-based suspension effectively reduces dynamic stresses, particularly under low-frequency excitations, while maintaining structural integrity and operational efficiency.

Keywords: vibro-isolation performance, nonlinear discrete model, kinematic excitations, quasi-zero stiffness, meta-structures.

1. Introduction

Vehicle ride quality constitutes a critical parameter for the secure and comfortable transportation of passengers and goods within automotive systems. For specific cargo types - such as vibration-sensitive or hazardous materials - it is essential to attenuate dynamic loads to mitigate the risk of damage or safety incidents. These dynamic stresses, which impact cargo, are primarily induced by road surface irregularities that propagate forces through the vehicle's wheels and suspension architecture. Non-linear suspension solutions, especially those designed with variable stiffness and damping properties [1,2], are therefore essential in modern automotive engineering, providing an optimal balance between vibration isolation and operational efficiency under varying conditions. By reducing dynamic loads, these systems not only improve stability and comfort for passengers, but also protect sensitive or dangerous loads from potential damage. This approach is particularly important on uneven road surfaces, where the forces transmitted through the suspension could otherwise create excessive stress on both passengers and loads.

In contemporary engineering practices, nonlinear suspension systems with adaptive stiffness or damping characteristics are extensively employed to suppress dynamic loads during transit. Among these, suspensions exhibiting quasi-zero stiffness (QZS) properties are particularly significant, as they afford effective vibration isolation while maintaining suspension efficacy. Such systems perform optimally under certain operational conditions and are advantageous for their compact configurations, which facilitate efficient spatial integration [3-6].

From engineering point of view QZS-elements could be realized with a different technical schema. For example, a Gas-Interconnected QZS pneumatic suspension is presented in the paper [7], [8] X-shaped structure is designed. The studies [9-11] examine various models of vibration isolators aimed at enhancing vibration isolation efficiency.

It is proposed to use an isolator consisting of *n* consecutive elements to study the mechanism of acquiring multiple characteristics of QZS in the paper [12]. Three types of equivalent mechanical models are studied the properties of the proposed isolator. It is found that with an increase in the number of layers, the proposed isolator is effective in achieving low-frequency vibration isolation at different preloads, and this advantage can be enhanced with small damping and excitation. A single-degree-of-freedom (DOF) system with the proposed isolator is created for theoretical and experimental study of its isolation characteristics in [12, 13]. The numerical method, through direct integration of the dynamic equation, verifies the analytical results of the frequency response functions. The experiment is carried out as well to verify the insulation performance of the nonlinear vibrator supported by the flexible plate.

Generally, one could sum up that negative stiffness, which arises in unit cells through buckling or snap-through, is considered the fundamental principle for energy absorption [5,10-12,14], i.e. by appropriately assembling unit cells with negative stiffness in series, in metamaterials and/or metastructures can be developed with desired shock protection or energy absorption performance [10,12]. Specially designed curved beams and inclined beams [5,10-12,14], placed under constrained supporting frames, are could be easy fabricate using 3D printing technology.

Based on the described different approaches one could find that the recent advances in meta-structures and additive technologies provide us with a new technologically efficient and cost-effective tools to realize QZS elements and integrate them into the suspension system of modern specialized vehicles.

A current study considers theoretical modeling of the dynamic behavior of a specialized vehicle with a dual suspension system. The first level is a typical torsion bar suspension with linear stiffness, while the second level has a nonlinear characteristic with a quasi-zero and a third vibration isolation/damping object, in particular with an internal elastic-damper support. The modeling is presented within the framework of numerical modeling of vibrations, which were analyzed based on a discrete nonlinear dynamic system. The dynamics of the system are analyzed with a kinematic impact load sequentially applied to the front and rear axles of the vehicle.

2. A discrete model of the specialized vehicle with nonlinear double-leveled suspension

A two-axle vehicle is considered, the model of which is shown in Fig. 1. It conditionally consists of three levels: basic suspension, platform and vibration isolation object. The vehicle base has a linear suspension, and the cargo platform has an additional suspension stage, which is connected to the 1st level of suspension with additional 2nd level that has a nonlinear elastic response with a quazy-zero stiffness (Fig. 1).

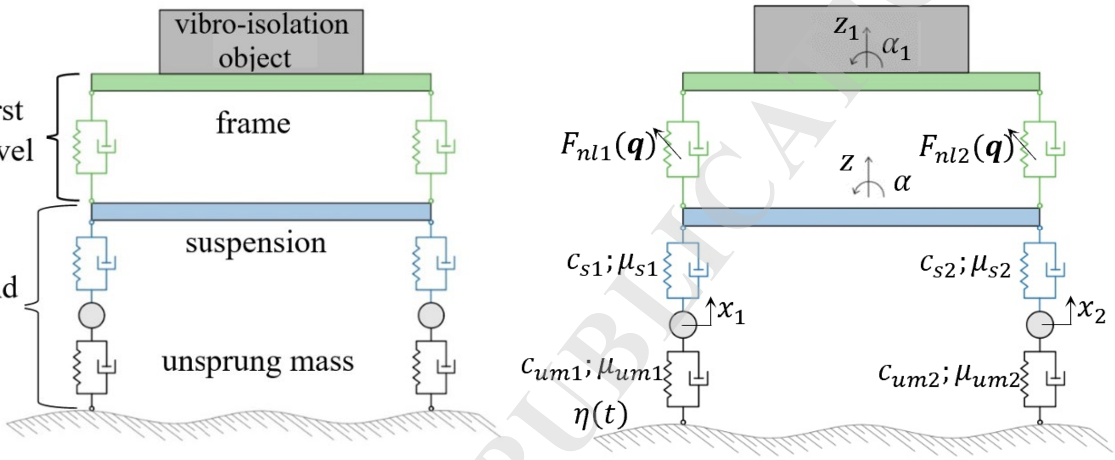

Fig. 1 – General schema of the proposed dynamic system that has double-levelled suspension

Lagrange's second order equation is used to develop a discrete nonlinear model according to the proposed vehicle design and shown on the Fig.1 its technical scheme

$$\frac{d}{dt}\left(\frac{\partial T}{\partial \dot{q}_i}\right) + \frac{\partial T}{\partial \dot{q}_i} + \frac{\partial \Pi}{\partial q_i} + \frac{\partial R}{\partial \dot{q}_i} = 0, \qquad i = \overline{1..6}, \tag{3}$$

where t is a time, T – kinetic energy of the system, Π – system potential energy, R - potential of the dissipative forces, q_i – generalized coordinates, which consist of masses vertical movements and angles of the rotations (4). The points placed above the functions indicates the time derivatives.

$$\{\boldsymbol{q}\} = \{x_1, x_2, z, \alpha, z_1, \alpha_1\}^T. \tag{4}$$

It is nothing difficult to get the kinetic energy

$$T = \frac{1}{2}\sum_{i=1}^{6} m_i \dot{q}_i^2, \tag{5}$$

where m_1 is a total front axle mass, that consist of two wheels and axle shaft, the same is for rare axle mass $m_2 = m_1$, m_3 is used to designates the total suspension mass (with all installed units) of the 1st level; $m_4 = m_{fr} + m_o$ is a total mass of 2nd level of suspension that includes cargo frame (m_{fr}) and the mass of the object of vibro-isolation (m_o). The moments of inertia of the 1st level frame as well as a frame of 2nd level (generally a specific cargo platform) are denoted as $m_5 = J_1$ and $m_6 = J_2$.

A system potential energy consists of potential energy for linear elastic elements (tires and first level of suspension) and of the potential energy of nonlinear suspension system of the second level:

$$\Pi = \Pi_l + \Pi_{nl}. \tag{6}$$

A linear part could be presented as follows:

$$\Pi_l = \frac{1}{2}\sum_{i=1}^{2} c_{umi}\big(x_i - \eta_i(t)\big)^2 + \frac{1}{2}\sum_{i=1}^{2} c_{si}(z - x_{1i})^2, \tag{7}$$

where the following designations are additionally used:

$$x_{11} = z - \frac{L}{2}\alpha, \quad x_{12} = z + \frac{L}{2}\alpha. \tag{8}$$

The potential energy of the second level suspension is defined as an integral of nonlinear elastic response, i.e. $F_{nl}(y) = \frac{\partial \Pi_{nl}}{\partial y}$. Considering that there are two nonlinear elements presented in the system (front and rear) the following equation for a Π_{nl} can be presented within the used on the Fig. 1 notations.

$$\Pi_{nl}(z, z_1, \alpha, \alpha_1) = \Pi_{nl1}(y_1 = z_1 - x_{21}) + \Pi_{nl2}(y_2 = z_1 - x_{22}), \tag{9}$$

where

$$x_{21} = z_1 - z + \frac{L}{2}(\alpha - \alpha_1), \quad x_{22} = z_1 - z + \frac{L}{2}(\alpha_1 - \alpha). \tag{10}$$

Considering the local and global coordinates correspondence the following formulations for a nonlinear forces could be proposed

$$F_3 = \frac{\partial \Pi_{nl1}}{\partial y_1}\frac{\partial y_1}{\partial z} + \frac{\partial \Pi_{nl2}}{\partial y_2}\frac{\partial y_2}{\partial z} = -[F_{nl}(y = z_1) + F_{nl}(y = z_2)], \tag{11}$$

$$\tilde{F}_3 = \frac{\partial \Pi_{nl1}}{\partial y_1}\frac{\partial y_1}{\partial \alpha} + \frac{\partial \Pi_{nl2}}{\partial y_2}\frac{\partial y_2}{\partial \alpha} = \frac{L}{2}[F_{nl}(y = z_1) - F_{nl}(y = z_2)], \tag{12}$$

$$F_4 = \frac{\partial \Pi_{nl1}}{\partial y_1}\frac{\partial y_1}{\partial z_1} + \frac{\partial \Pi_{nl2}}{\partial y_2}\frac{\partial y_2}{\partial z_1} = F_{nl}(y = z_1) + F_{nl}(y = z_2), \tag{13}$$

$$\tilde{F}_4 = \frac{\partial \Pi_{nl1}}{\partial y_1}\frac{\partial y_1}{\partial \alpha_1} + \frac{\partial \Pi_{nl2}}{\partial y_2}\frac{\partial y_2}{\partial \alpha_1} = \frac{L}{2}[-F_{nl}(y = z_1) + F_{nl}(y = z_2)]. \tag{14}$$

Dissipative forces in the current study is proposed to be considered within a Raleigh linear model in the where damping matrix is proportional to linear stiffness matrix, wherefor the damping potential is a quadratic form of general coordinates velocities

Substituting (5) and (6) considering (7) - (14) in the Lagrange equation (3) one can obtain the main system of equations (15).

$$\begin{cases} m_1\ddot{x}_1 + \frac{\partial R}{\partial \dot{x}_1} + F_{el1} = c_t\eta_1(t), \\ m_2\ddot{x}_2 + \frac{\partial R}{\partial \dot{x}_2} + F_{el2} = c_t\eta_2(t), \\ m_3\ddot{z} + \frac{\partial R}{\partial \dot{z}} + F_{el3} + F_3(z, z_1, \alpha, \alpha_1) = 0, \\ J_1\ddot{\alpha} + \frac{\partial R}{\partial \dot{\alpha}} + F_{el4} + \tilde{F}_3(z, z_1, \alpha, \alpha_1) = 0, \\ m_4\ddot{z}_1 + \frac{\partial R}{\partial \dot{z}_1} + F_4(z, z_1, \alpha, \alpha_1) = 0, \\ J_2\ddot{\alpha}_1 + \frac{\partial R}{\partial \dot{\alpha}_1} + \tilde{F}_4(z, z_1, \alpha, \alpha_1) = 0. \end{cases} \tag{15}$$

Thus, we have the system of differential equations describing the dynamics of the vehicle, which has a double-level nonlinear suspension, where the 2nd level is additional and has a nonlinear characteristic. In the system (15) for simplification of presented from of equations a vector of elastic forces (F_{el}) is introduced

$$\{\boldsymbol{F}_{el}\} = [\boldsymbol{K}]\{\boldsymbol{q}\}, \tag{16}$$

$$[\boldsymbol{K}] = \begin{bmatrix} (c_{um1} + c_{s1}) & 0 & -c_{s1} & {}^{L}/_{2}\, c_{s1} & 0 & 0 \\ & (c_{um2} + c_{s2}) & -c_{s2} & -{}^{L}/_{2}\, c_{s2} & 0 & 0 \\ & & c_{ss} & -{}^{L}/_{2}\, c_{sn} & 0 & 0 \\ & & & L^2\, {}^{c_{ss}}/_{4} & 0 & 0 \\ & symmetric\ part & & & 4c_{fr} & 0 \\ & & & & & L^2 c_{fr} \end{bmatrix}, \tag{17}$$

where for a simplification we introduced additional parameters for the total stiffness of first level of suspension and for the difference between the front and rear axles part of stiffness of first level suspension:

$$c_{ss} = c_{sn1} + c_{sn2},\ c_{sn} = c_{sn2} - c_{sn1}. \tag{18}$$

In the matrix of stiffness an additional parameter c_{fr} is introduced. It is artificially added as a linearized (through bisection approximation) stiffness of the 2nd level of suspension. Derived elastic forces F_{el5} and F_{el6} are not used in the equations (15) directly, but the stiffness matrix in the total size is used for the introduction of damping and for some calculations of the natural frequencies and normal modes that are used for model testing and basic preliminary dynamic analysis.

Also, the system of equations (15) has some dissipative forces, which are reflect the presence of the viscosity of tire deformation and the damping in the first level of suspension.

These forces are derived from a corresponding potential of dissipative forces (11) and have the following analytical expressions, given bellow in a matrix form:

$$\left\{\frac{\partial R}{\partial \dot{q}}\right\} = \mu[\boldsymbol{K}]\{\dot{\boldsymbol{q}}\}. \tag{19}$$

The system (15) affords to analyze vertical and angular vibrations of the vehicle occurring under the kinematic excitations $\eta_1(t)$ and $\eta_2(t)$, which are applied to the wheels of the vehicle due to the interaction with the road surface roughness. Herewith, it must be underlined that a time delay must be taken into account then the kinematic load is applied

$$\eta_1(t) = \eta(t), \ \ \eta_2(t) = \eta\left(t + \frac{L}{v}\right), \tag{20}$$

where L is the distance between the wheel axles, v is the vehicle riding speed.

A simple perturbation is introducing here as a half-sinusoidal function of time:

$$\eta(t) = \begin{cases} a_0 \sin \frac{\pi(t-t_0)}{t_n - t_0}, t \in [t_0, t_n] \\ 0, t \notin [t_0, t_n] \end{cases}, \tag{21}$$

where a_0 is a amplitude (high) of the geometric perturbation, t_0, t_n - initial and final moment of time where the perturbation is in action. t_n – is calculated from the geometric size of perturbation (width) and a velocity of vehicle ride.

Presented system of equation (15) is identified with the nonlinear elastic forces $F_{nl}(y)$. In the current work we propose to used a specific element that has a quazy-zero stiffness (QZS) of its elastic response. In the study we had numerical identified such a response of QZS-element and approximate that dependencies using cubic splines. Some details of this element modeling is presented below.

3. An integral nonlinear elastic response of the QZS-element

Following the idea of meta-materials repetitive elementary cell proposed in the paper [10] in the current study we used the QZS elements, that is formed by a sinusoidal beam, a pair of semicircular arches, and stiffer wall elements.

The 3D model was build in parametric form that allow us to find a rational geometrical parameters of the QZS-element, that has a quasy-zero stiffness response region within a required range of possible displacements as well as the required from the practical point of view the level of response forces, that allow us to used such an element for real applications. Finite element (FE) modeling is used for direct computer simulations that allow us to obtain an integral elastic response of the QZS-element under the kinematic (displacement control) loading. Fig. 2 represents geometry and FE mesh.

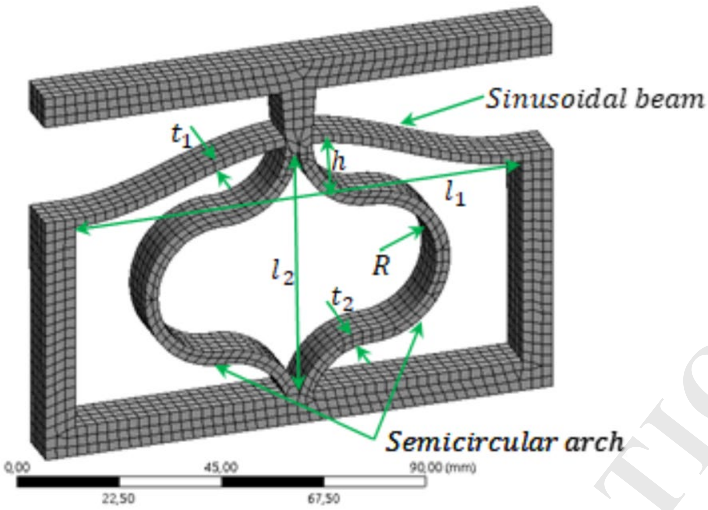

Fig. 2 QZS- element FE model and geometry

Final mode parameters allow us to obtain the nonlinear characteristic of the QZS-element that has almost zero reaction on the displacement perturbations in the region of 30 mm, correspondent results of computer simulations presented in the Fig. 3.

The main geometric parameters of the QZS-element that is figure out form a set of FE simulations and used as a basic model in the current paper are the following: l_1 = 208 mm (width), l_2 = 120 mm (hight), l_3 = 14 mm (thickness); t_1 = 8,1 mm (“beam“ thickness), t_2 = 12,4 mm (“arc“ thickness); h = 31,5 mm; R =30 mm.

It should be noted that if the potential displacements exceed the specified values, the stiffness of this system will lead to the opposite effect in terms of vibration isolation. This unit element demonstrates satisfactory results and can serve as a basis for modeling a more complex vibration isolator that can operate at higher displacement levels. Fig. 3 shows these results, which are cantered around a zero considering mean-basic static load.

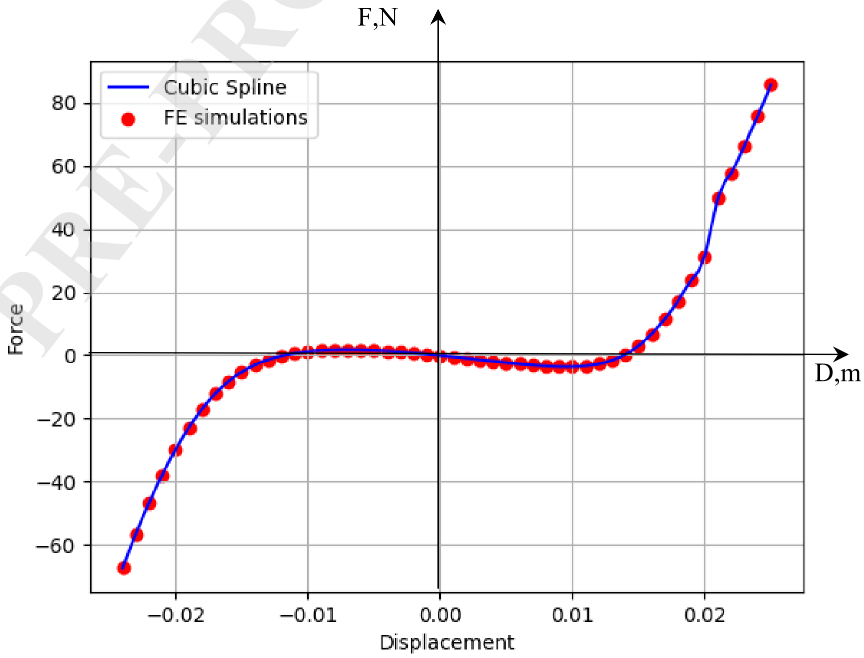

Fig. 3 Integral nonlinear elastic response of QZS-element

FE simulation allow us to find and analyses additional the strength parameters of the QZS-element. The last is important from the practical point of reliability ensuring. Fig. 4 demonstrates the distributions of displacements (deformation filed) and von-Mises stresses at the different level of displacement control load with ± 9 mm.

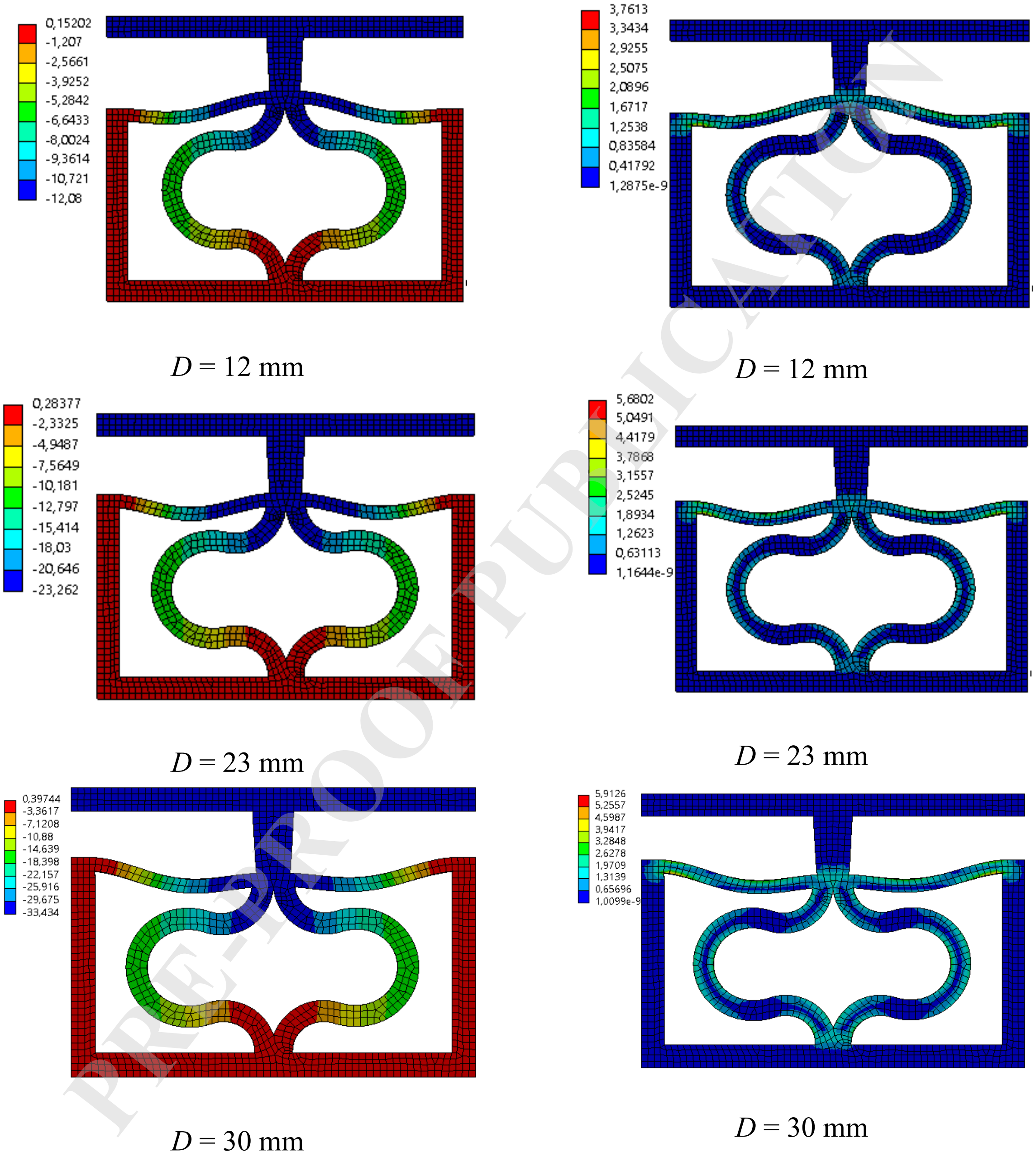

a) b)

Fig.4 a) Vertical displacements (mm); b) equivalent von Mises stresses (MPa) for different levels of load displacements

4. Results of the numerical simulations of vibro-isolation performance for sensitive cargo transportation

Presented in the section 2 mathematical model with identified from the direct FE simulations nonlinear elastic responses (F_{nl}) of QZS-elements is used for numerical computations of the dynamics of such a system. Differential equations (15) in this paper are solving numerically within an explicit integration scheme. Mechanical and geometrical parameters that are used in the numerical experiments are summarized in a Table 1.

Table 1. Mechanical parameters of the system

parameter	L	m_1, m_2	m_3	m_4
units	m	kg	kg	kg
value	2,2	83	168	176
parameter	I_1	I_2	c_{sn1}, c_{sn2}	c_{um}
units	kg ·m^2	kg ·m^2	kN/m	kN/m
value	252,3	344,6	240	350

As a results of integrations, we have been found the dynamic of displacements of all general coordinates as well as velocities and accelerations. Fig. 5 and Fig. 6 presents an example of the time dependencies that were computed for the vertical vibrations on a front and rear axes, vertical vibrations of the center of mass at the 1st and 2nd of suspension, i.e. z and z_1. For the current example here the case of the overriding of the road roughness with the high of 50 mm and the width of 300 mm (standard road).

These results presented for the case where 2nd level of suspension is excluded from the model. Technically, that realize by the substitution of nonlinear forces with linear one with an extreme huge stiffness (10^8 N/m – corresponds to the stiff metal rod connection between the suspension levels. Such a trick approach allow us to keep the same mass-inertial properties in the both models: basic linear (Model L) and double-levelled nonlinear (Model NL)).

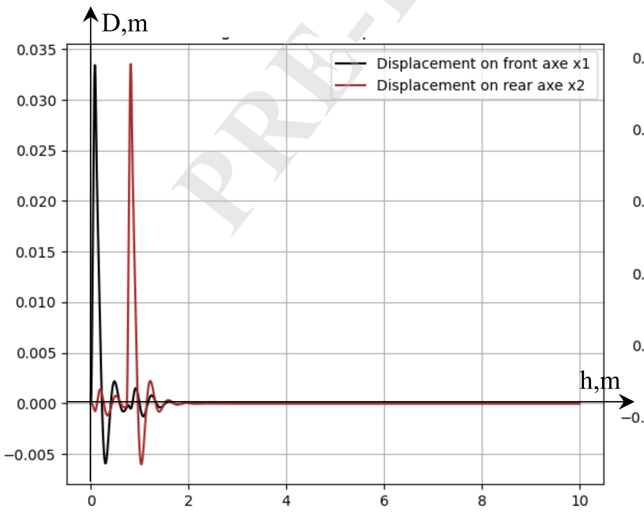

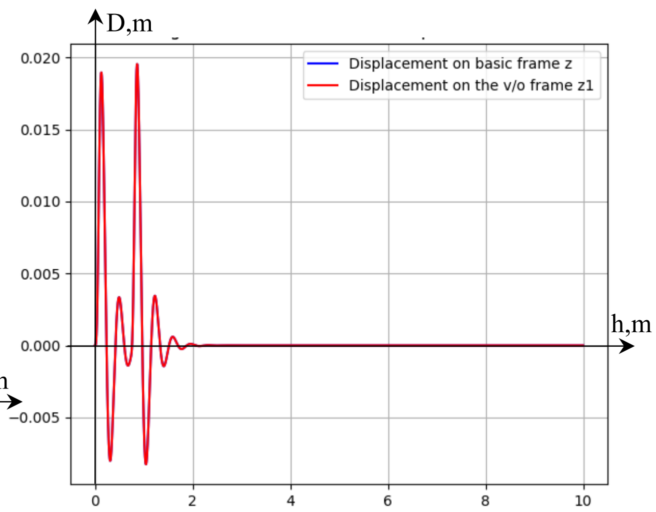

Fig. 5 Vertical vibrations of the generalize coordinates of vehicle without a 2nd level of nonlinear suspension (Model L)

Fig.6 shows time dependencies of the level of vibro-velocities and vibro-accelerations in the centre of mass of the cargo object (object of potential vibro-isolations) for the Model L.

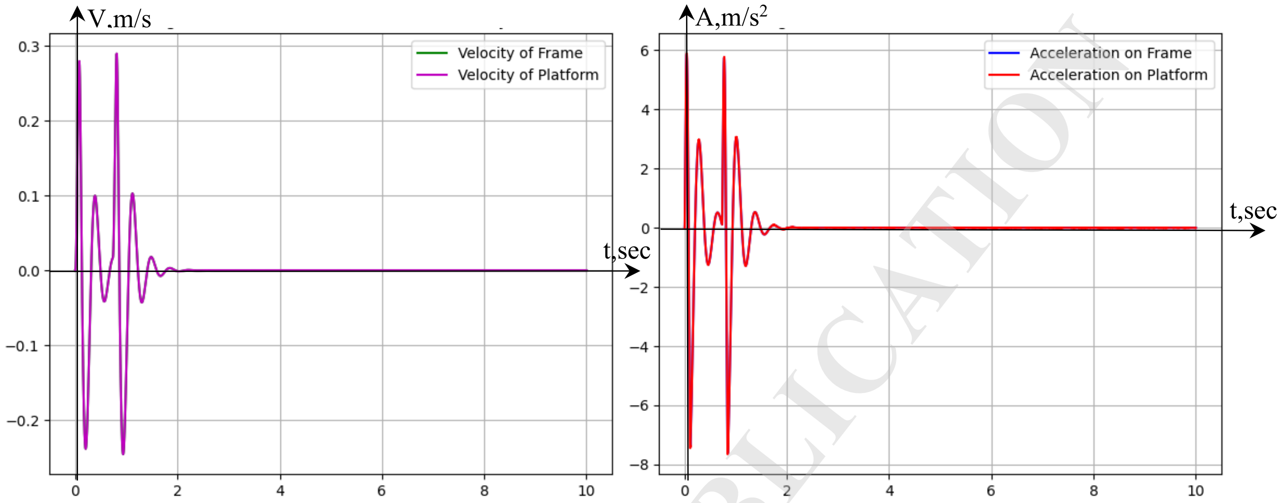

Fig. 6 Vertical velocities and accelerations of the center mass of the cargo object

The same results have been obtained for the proposed system that have a 2nd level of suspension with integrated nonlinear QZS elements (Model NL). Fig. 7 and Fig. 8 show results for this second case. Vertical vibrations on the axes have the similar behavior and the same amplitudes levels as well as a vertical dynamic of the center of masses of 1st level of suspension. However, the second level center of masses that actually corresponds to the cargo object (object of vibro-isolation) has significant reduction of amplitudes of vibrations at the moments of impacts. An interesting phenomena is also observed, that a displacement (position) of the object center of masses has smooth shifting over a time after the impacts influence. Perhaps this post-action peculiarity caused with inertia influence and shows some negative phenomena of energy accumulation in the QZS-elements.

Analysis of the level of vibro-velocities and vibro-accelerations shows a triple reduction of the amplitude levels. The last approve a crucial efficiency of the integration of QZS elements with an additional level of suspension.

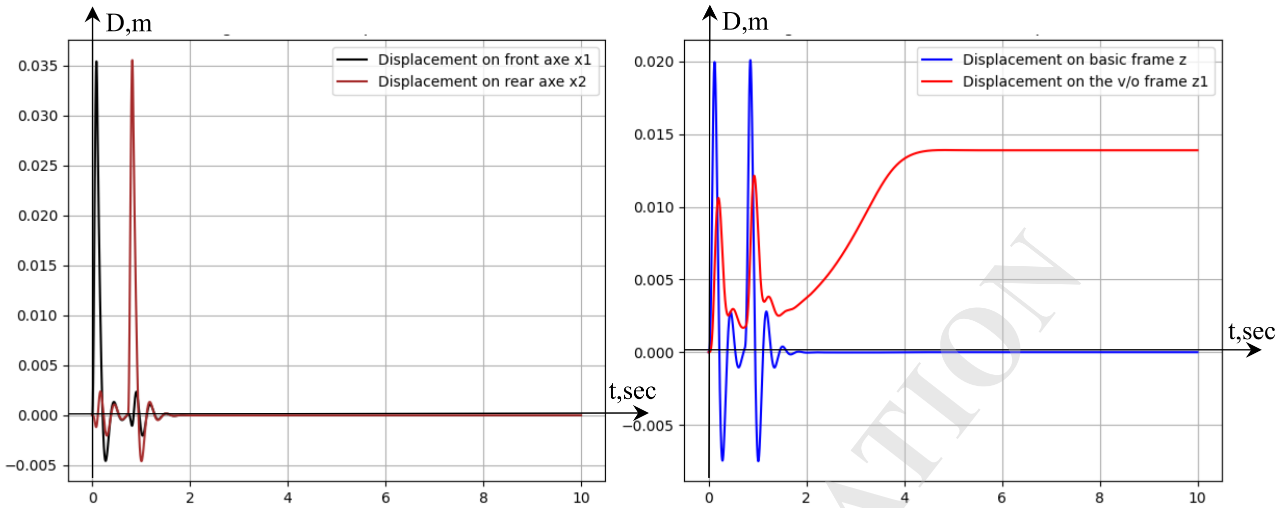

Fig. 7 Vertical vibrations of the generalize coordinates of vehicle with a 2nd level of nonlinear suspension (Model NL)

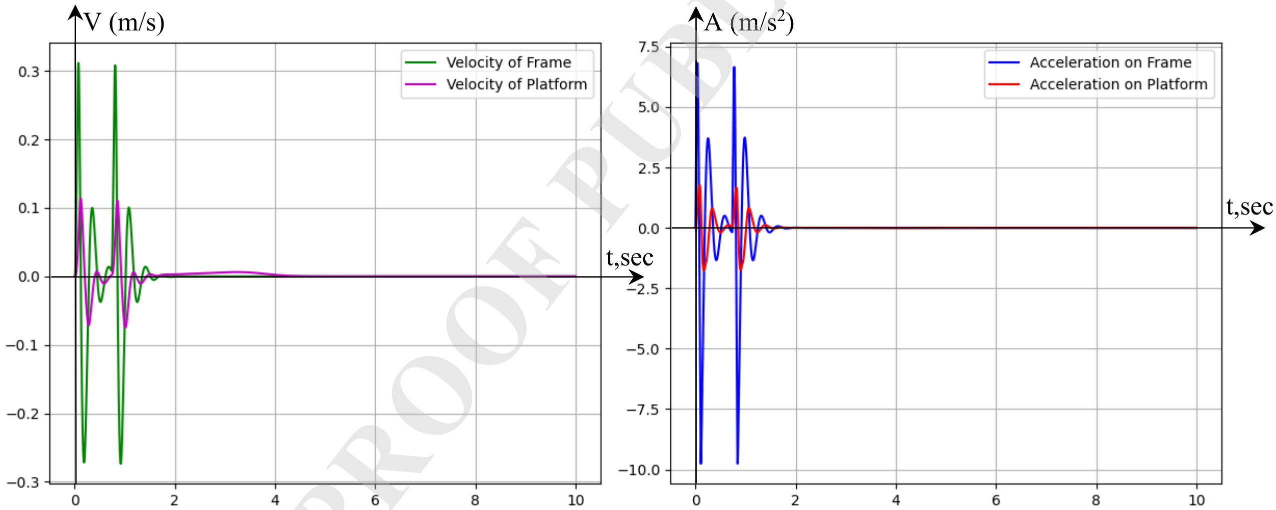

Fig. 8 Vertical vibrations of the generalize coordinates of vehicle with a 2nd level of nonlinear suspension (Model NL)

Within a current study seria of comparative computations have been carried out for analysis of the vertical vibrations (displacements, velocities and accelerations) with a variation of the level and shape of kinematic impacts. We have varied the amplitude of the impact (the high of road roughness) in the range from 10 mm to 100 mm but with a fixed time of impact (overriding with a constant riding speed that correspondent road roughness with 300 mm width). The results of the calculations visualized on the Fig. 9. Proposed system of vibro-isolations shows us a good efficiency over amplitudes of vertical vibration for the impact with amplitudes up to 70 mm with maximum of its efficiency at 100% amplitude reduction. On the Fig. 9 a phase tracks of vertical vibration are additional plotted.

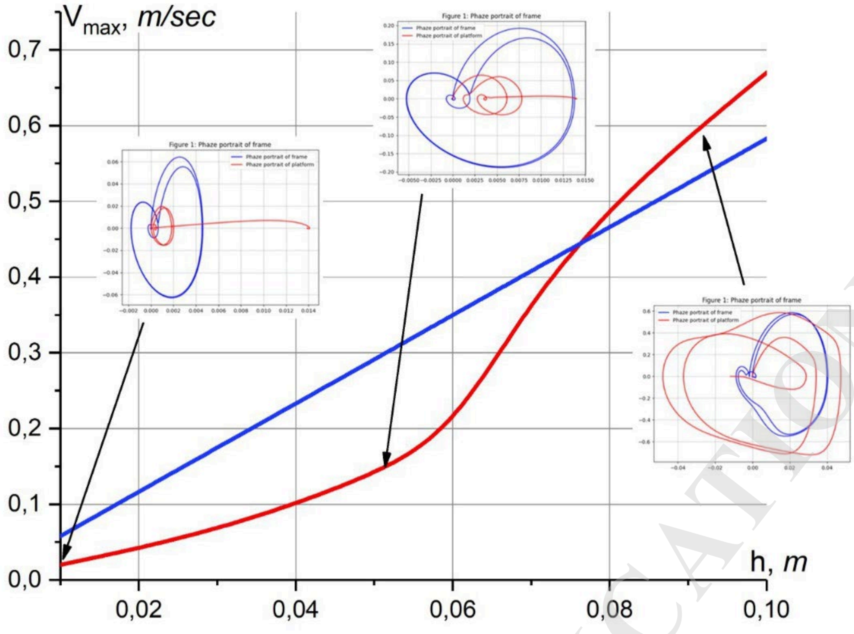

Fig. 9 Vertical vibrations of the point of center of masses of vibro-isolated object (Model L is a blue line; Model NL is a red line)

Additional we examined the influence of the impact width on the vibro-isolation performance. Results presented on the Fig. 10 and Fig. 11. Shows that with increasing road roughness width, the amplitudes of vibro-velocities and vibro-accelerations rise in the nonlinear model, whereas they reduce linearly and slightly in the linear model. Despite this, the nonlinear model consistently demonstrates good efficiency up to 90 mm road roughness height. For instance, at a 60 mm impact height and 0.6 m width, we observed a two-fold reduction in vibro-accelerations.

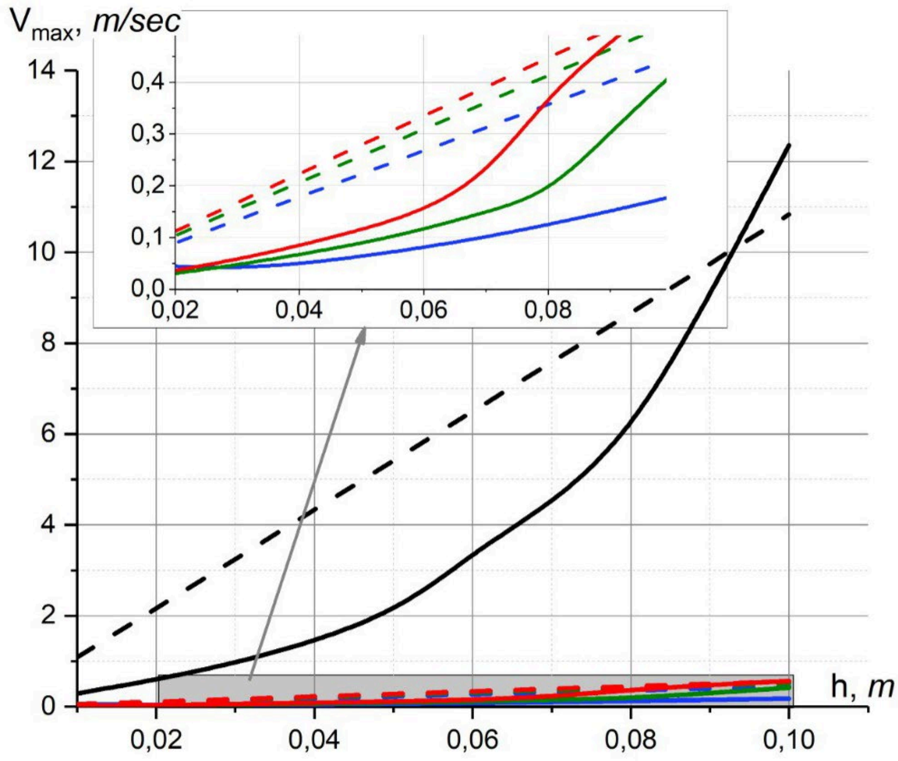

Fig. 10 Vertical vibro-velocities of the point of center of masses of vibro-isolated object on dependence of kinematic impact width (Model L is a dash line; Model NL is a solid line)

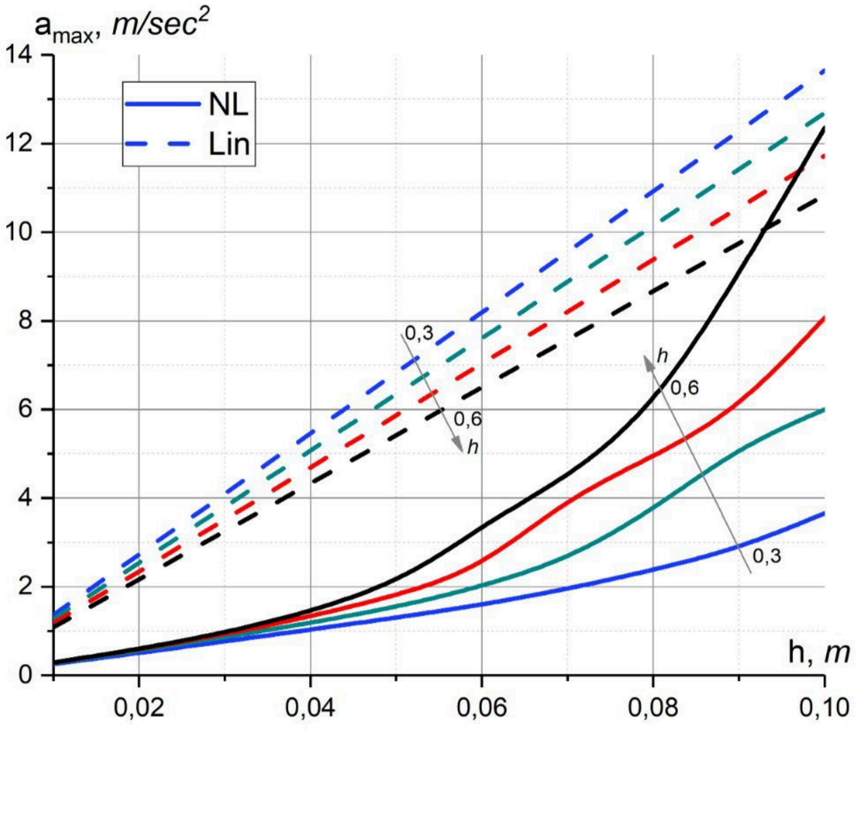

Fig. 11 Vertical accelerations of the point of center of masses of vibro-isolated object on dependence of kinematic impact width (Model L is a dash line; Model NL is a solid line)

5. Conclusion

The presented study highlights the advancements in suspension systems for specialised vehicles, emphasising the integration of nonlinear and quasi-zero stiffness (QZS) elements to enhance ride quality and vibration isolation. By combining linear and nonlinear suspension levels, the proposed dual-suspension system effectively minimizes dynamic loads, safeguarding passengers and cargo. Leveraging modern meta-structural designs and additive manufacturing, the system achieves cost-efficient and compact configurations suitable for various operational conditions.

Numerical simulations demonstrate the significant effectiveness of the QZS-integrated suspension system. We observed a three-fold reduction in amplitude levels for vibro-velocities and vibro-accelerations when comparing the QZS model to the basic linear model. The system effectively reduces vertical vibration amplitudes for kinematic impacts up to 70 mm in height.

The intriguing phenomenon: after impacts, the displacement (position) of the object's centre of mass exhibits a smooth, prolonged shift over time. This post-action peculiarity, likely due to inertial influences, suggests a potential negative phenomenon of energy accumulation within the QZS-elements. For better system behaviour in operational scenarios, perhaps, a system of automatic positioning and specific control will need to be developed.

Author agreement

The authors have reviewed and approved the final version of the manuscript submitted for publication. They warrant that this article is their original work, has not been previously published and is not currently under consideration for publication elsewhere.

Conflicts of interest

The authors declare that there are no conflicts of interest associated with this study.

Funding

This scientific study was supported and partially funded by National Research Foundation of Ukraine (NRFU grant number 2023.03/0255).

Data availability statement

Some or all of the data, models, or code that support the findings of this study are available from the corresponding author upon request.

References

1. Yang Jin, Shuai Hou, Tianzhi Yang *Cascaded essential nonlinearities for enhanced vibration suppression and energy harvesting* Nonlinear Dynamics, 103, p. 1427–1438, 2021. https://doi.org/10.1007/s11071-020-06165-6
2. Fidrovska N., Slepuzhnikov E., Larin O., Afanasenko K., Harbuz S. *Increase of operating reliability of the travel wheel using the use of the elastic inserts* EUREKA, Physics and Engineering, 2020(5), pp. 69–79, 2020 https://doi.org/10.21303/2461-4262.2020.001387
3. Kai Wang, Jiaxi Zhou, Yaopeng Chang, Huajiang Ouyang, Daolin Xu & Yang Yang *A nonlinear ultra-low-frequency vibration isolator with dual quasi-zero-stiffness mechanism,* Nonlinear Dynamics, Volume 101, p 755–773, 2020. https://link.springer.com/article/10.1007/s11071-020-05806-0
4. Bo Yan , Ning Yu , Hongye Ma , Chuanyu Wu *A theory for bistable vibration isolators* Mechanical Systems and Signal Processing, Volume 167, Part A, 2022. https://doi.org/10.1016/j.ymssp.2021.108507
5. Bo Yan, Zhihao Wang, Hongye Ma, Huihuang Bao, Ke Wang, Chuanyu Wu *A novel lever-type vibration isolator with eddy current damping,* Journal of Sound and Vibration, Volume 494, 2021. https://doi.org/10.1016/j.jsv.2020.115862
6. Jing Bian & Xingjian Jing *Analysis and design of a novel and compact X-structured vibration isolation mount (X-Mount) with wider quasi-zero-stiffness range*, Nonlinear Dynamics, 101, p. 2195–2222, 2020. https://link.springer.com/article/10.1007/s11071-020-05878-y
7. Xinwei Jiang, Xing Xu, Tianling Shi & Vincent Akolbire Atindana *Nonlinear Characteristic Analysis of Gas-Interconnected Quasi-Zero Stiffness Pneumatic Suspension System: A Theoretical and Experimental Study,* Chinese Journal of Mechanical Engineering, volume 37, 58, 2024. https://cjme.springeropen.com/articles/10.1186/s10033-024-01039-z
8. Huayan Pu [a b], Shujin Yuan [a], Yan Peng [a], Kai Meng [a c], Jinglei Zhao [a], Rongqing Xie [a], Yining Huang [a], Yi Sun [a b], Yang Yang [a], Shaorong Xie [a], Jun Luo [a], Xuedong Chen [b] *Multi-layer electromagnetic spring with tunable negative stiffness for semi-active vibration isolation,* Mechanical Systems and Signal Processing, Volume 121, PP. 942-960, 2019. https://doi.org/10.1016/j.ymssp.2018.12.028
9. Ze-Qi Lu,Dong-Hao Gu,Hu Ding,Walter Lacarbonara,Li-Qun Chen *Nonlinear vibration isolation via a circular ring,* Mechanical Systems and Signal Processing, Volume 136, 2020. https://doi.org/10.1016/j.ymssp.2019.106490
10. Haigui Fan, Lijuan Yang, Yuchen Tian & Zewu Wang, *Design of metastructures with quasi-zero dynamic stiffness for vibration isolation*, Composite Structures, Volume 243, 2020, 112244. https://doi.org/10.1016/j.compstruct.2020.112244
11. Mohaddeseh Gholikord, Ehsan Etemadi, Mohammad Imani & Mahboubeh Hosseinabadi, *Design and analysis of novel negative stiffness structures with significant energy absorption*, Thin-Walled Structures, Volume 181, 2022, 110137. https://doi.org/10.1016/j.tws.2022.110137

12. Srajan Dalela, P. S. Balaji, Moussa Leblouba, Suverna Trivedi & Abul Kalam, *Nonlinear static and dynamic response of a metastructure exhibiting quasi-zero-stiffness characteristics for vibration control: an experimental validation*, Scientific Reports, Volume 14, 19195, 2024. https://doi.org/10.1038/s41598-024-70126-x

13. Rong-Biao Hao, Ze-Qi Lu, Hu Ding & Li-Qun Chen *A nonlinear vibration isolator supported on a flexible plate: analysis and experiment*, Nonlinear Dynamics, 108, p. 941–958, 2022. https://link.springer.com/article/10.1007/s11071-022-07243-7

14. David A. Debeau, Carolyn C. Seepersad & Michael R. Haberman, *Impact behavior of negative stiffness honeycomb materials*, Mechanical Engineering Department, The University of Texas at Austin, Austin, Texas 78712, USA.